Targeting Solid Cancers with a Cancer-Specific Monoclonal Antibody to Surface Expressed Aberrantly *O*-glycosylated Proteins

Mikkel K.M. Aasted[1], Aaron C. Groen[2], John T. Keane[3], Sally Dabelsteen[4], Edwin Tan[2], Julia Schnabel[2], Fang Liu[3], Hyeon-Gyu S. Lewis[3], Constantine Theodoropulos[2], Avery D. Posey Jr[3,5], and Hans H. Wandall[1,2]

ABSTRACT

The lack of antibodies with sufficient cancer selectivity is currently limiting the treatment of solid tumors by immunotherapies. Most current immunotherapeutic targets are tumor-associated antigens that are also found in healthy tissues and often do not display sufficient cancer selectivity to be used as targets for potent antibody-based immunotherapeutic treatments, such as chimeric antigen receptor (CAR) T cells. Many solid tumors, however, display aberrant glycosylation that results in expression of tumor-associated carbohydrate antigens that are distinct from healthy tissues. Targeting aberrantly glycosylated glycopeptide epitopes within existing or novel glycoprotein targets may provide the cancer selectivity needed for immunotherapy of solid tumors. However, to date only a few such glycopeptide epitopes have been targeted. Here, we used *O*-glycoproteomics data from multiple cell lines to identify a glycopeptide epitope in CD44v6, a cancer-associated CD44 isoform, and developed a cancer-specific mAb, 4C8, through a glycopeptide immunization strategy. 4C8 selectively binds to Tn-glycosylated CD44v6 in a site-specific manner with low nanomolar affinity. 4C8 was shown to be highly cancer specific by IHC of sections from multiple healthy and cancerous tissues. 4C8 CAR T cells demonstrated target-specific cytotoxicity *in vitro* and significant tumor regression and increased survival *in vivo*. Importantly, 4C8 CAR T cells were able to selectively kill target cells in a mixed organotypic skin cancer model having abundant CD44v6 expression without affecting healthy keratinocytes, indicating tolerability and safety.

Introduction

Immunotherapeutic strategies, such as chimeric antigen receptor (CAR) T cells, bispecific T-cell engagers, and antibody–drug conjugates (ADC), have emerged as potent tools in cancer treatments. In hematological cancers, CAR T cells have achieved great success likely due to the accessibility of the cancer cells and the general tolerability of off-target effects, as in the case of CD19-targeting CAR T cells in B-cell malignancies (1–5). However, the adaptation of CAR T-cell therapies to carcinomas has been troublesome. Apart from anatomical inaccessibility and an immunosuppressive tumor microenvironment, carcinomas often lack suitable antigens as severe off-target toxicity may occur even with minimal antigen expression in healthy epithelia (6). Therefore, to facilitate the future use of potent immunotherapies as CAR T cells in solid tumors it is necessary to identify highly selective cancer-specific antigens.

A promising strategy to identify novel cancer-specific antigens is the utilization of aberrant glycosylation, which is a feature unique to- and shared by many cancers (7–11). Aberrant glycosylation has been described as a hallmark of cancer due to its abundance in cancers and its direct involvement in carcinogenesis and cancer progression (12, 13). Glycosylation is an abundant post-translational modification that involves the covalent attachment of carbohydrate structures, called glycans, to glycoproteins and glycolipids. There are several types of protein glycosylation, but most abundant is the *N*-linked glycosylation and the GalNAc type *O*-linked glycosylation, hereafter simply called *O*-glycosylation (14). Cancer-associated changes in *O*-glycans include truncation, resulting in expression of the immature Tn (GalNAcα1-*O*-Ser/Thr), STn (NeuAcα2–6GalNAcα1-*O*-Ser/Thr), and T (Galβ1–3GalNAcα1-*O*-Ser/Thr) antigens (7, 8, 15–17). Truncated *O*-glycans are particularly interesting as they are observed in most carcinomas (11, 18–20) and correlate with poor clinical outcomes and cancer progression (21–24). In addition, it is becoming increasingly clear that truncated *O*-glycans have pivotal roles in carcinogenesis, as they directly induce oncogenic features, including altered differentiation, impaired adhesion, and increased invasion (25–31). We have previously identified human *O*-glycopeptide epitopes and successfully demonstrated their use in the detection and targeting of cancer cells (32–35). Thus, *O*-glycopeptide epitopes composed of a truncated *O*-glycan and a short peptide sequence show promise as true cancer-specific antigens, but up until now, only few glycopeptide epitopes have been targeted. Over the last years, we have greatly expanded the known human *O*-glycoproteome through glycoproteomics analyses of various cell and tissue samples to more than 10.000 *O*-glycosylation sites (31, 36–38). In this study, we used this development to target a glycopeptide epitope in CD44v6 (GYRQTPKEDSHS(Tn)TTGTAAA) that is glycosylated across cancer cell lines.

[1]Department of Cellular and Molecular Medicine, Copenhagen Center for Glycomics, University of Copenhagen, Copenhagen, Denmark. [2]GO-Therapeutics, One Broadway, Cambridge, Massachusetts. [3]Department of Systems Pharmacology and Translational Therapeutics, Perelman School of Medicine, University of Pennsylvania, Philadelphia, Pennsylvania. [4]Department of Oral Pathology, School of Dentistry, University of Copenhagen, Copenhagen, Denmark. [5]Corporal Michael J. Crescenz VA Medical Center, Philadelphia, Pennsylvania.

M.K.M. Aasted and A.C. Groen contributed equally as co-authors of this article.

Corresponding Authors: Hans H. Wandall, University of Copenhagen, Blegdamsvej 3, Copenhagen, 2200 N, Denmark. E-mail: hhw@sund.ku.dk and hans@gotherapeutics.com; and Avery D. Posey, aposey@pennmedicine.upenn.edu

Mol Cancer Ther 2023;22:1204–14

doi: 10.1158/1535-7163.MCT-23-0221

CD44v6 is a cancer-associated isoform of the highly glycosylated transmembrane protein CD44 that has been clinically targeted in squamous cell carcinomas by the ADC bivatuzumab mertansine, but failed due to severe skin toxicities (39–42). We identified one mAb, 4C8, highly specific for Tn-glycosylated epitopes and selectively stains tumor tissues. Developed into CAR T cells, 4C8 demonstrated Tn-dependent cytotoxicity *in vitro* and *in vivo* and selectively killed Tn-expressing cancer cells in a human organotypic skin tumor model. These findings demonstrate the efficacy and safety of the glycopeptide targeting 4C8 mAb and highlight the potential to expand the current number of selective cancer targets in carcinomas.

Materials and Methods

Cell culture

Human male colorectal carcinoma cell line HCT 116 (RRID: CVCL_0291), human embryonic kidney (HEK) 293T (RRID: CVCL_0063), human male immortalized keratinocyte cell line HaCaT (RRID:CVCL_0038), human female Ewing sarcoma cell line A-673 (RRID:CVCL_0080), and human male lung carcinoma cell line A549 (RRID:CVCL_0023) were cultured in DMEM supplemented with 10% FBS. Human female breast carcinoma cell line MCF7 (RRID: CVCL_0031) was cultured in DMEM supplemented with 10% FBS and 10 μg/mL human recombinant insulin. Human female breast carcinoma cell line T-47D (RRID: CVCL_0553), human male pancreatic carcinoma cell line T3M-4 (RRID:CVCL_4056), and human male T-cell leukemia cell line Jurkat (RRID: CLCL_0065) were cultured in RPMI-1640 supplemented with 10% FBS. Human male immortalized keratinocyte cell line N/TERT-1 (RRID:CVCL_CW92) was cultured in Keratinocyte Serum Free Medium (KSFM) supplemented with 25 mg/mL BPE (Gibco), 0.2 ng/mL EGF (Thermo Fisher Scientific), and 0.3 mmol/L CaCl2 (Sigma). All cells were maintained in humidified incubators at 37°C with 5% CO_2 and were regularly tested for *Mycoplasma* using MycoStrip (InvivoGen). Cell line authentication was not performed but the cell lines were monitored for correct morphology and phenotypic behavior. COSMC knockout (KO) cell lines were previously generated in our laboratory using CRISPR/Cas9.

Generation of mAbs

Synthesis of O-glycopeptide CD44v6Tn

CD44v6 *O*-glycopeptide with the sequence GYRQTPKEDSHS-TTGTAAA was synthesized using standard FMOC peptide synthesis strategy. Pre-synthesized glycosylated amino acids were coupled to the elongating peptide at threonine 5, serine 12, or both, using solid or solution phase peptide chemistry in a stepwise fashion. After completing the full sequence and removing all protecting groups, the resulting glycopeptide was purified by high-performance liquid chromatography and characterized by mass spectrometry (electrospray ionization in positive mode).

Immunization and fusion

Female Balb/c mice were immunized subcutaneously with CD44v6-Tn(S12) glycopeptide conjugated to keyhole limpet hemocyanin (KLH) through a glutaraldehyde linker. The mice were immunized on days 0, 14, and 35 with 50, 45, and 45 μg of KLH-glycopeptide, respectively. The first immunization used Freund's complete adjuvant. All subsequent immunizations used Freund's incomplete adjuvant. On day 45, tail bleeds were evaluated for polyclonal response. On day 56 or after, mice with a positive polyclonal response were boosted with 15 μg of KLH-glycopeptide in Freund's incomplete adjuvant 3 to 5 days before hybridoma fusion. Splenocytes from mice were fused with SP2/0-Ag14 (ATCC, cat# CRL-1581) myeloma cells using the Electro Cell Manipulator (ECM2001) from BTX Harvard Apparatus. Hybridomas were seeded in 96-well plates, cultured, scaled, and evaluated and selected for specificity toward CD44v6-Tn using ELISA, flow cytometry, and immunofluorescence until mAbs were obtained.

Characterization of antibodies

ELISA

96-well Corning high-bind microplates (Thermo Fisher Scientific) were coated overnight at 4°C with various concentrations of naked CD44v6, CD44v6-Tn(T5), CD44v6-Tn(S12), CD44v6-Tn(T5+S12), and unrelated peptides in 0.2 mol/L bicarbonate-carbonate buffer (pH 9.4). The plates were then blocked for 1 hour at room temperature with PBS (pH 7.4) containing 2.5% BSA. Contents of the plate were discarded and purified antibody, hybridoma supernatants, or blood serum to be probed for polyclonal responses, were added at various concentrations and incubated for two hours at room temperature. Plates were washed with TBS with 0.05% Tween-20 and then incubated for 1 hour at room temperature with a 1:3,000 dilution of horseradish peroxidase (HRP)–conjugated goat anti-mouse IgG Fcγ (Sigma). The plates were washed again and developed with TMB chromogen substrate. After proper development (approximately 2–3 minutes), the reaction was stopped with 0.2 N H_2SO_4 and the absorbance was read at 450 nm. Data were analyzed in GraphPad Prism Software.

Flow cytometry

Adherent cells were dissociated with TrypLE select (Gibco) and washed from flask surface with cell culture media (RPMI with 2 mmol/L L-glutamine, 1% PenStrep, and 10% FBS). Cells were washed several times by centrifugation at 300 × *g* for 5 minutes at 4°C followed by resuspension in PBS with 1% BSA (PBS/1%BSA). Cells were resuspended between a total of 5×10^5 and 2×10^6 cell/mL and then distributed into a 96-well U-bottom plate. Diluted commercial CD44v6 antibody (0.25–2 μg/mL; Thermo Fisher Scientific), biotinylated VVA-lectin (2 μg/mL; Vector Laboratories), hybridoma supernatants, or blood serum to be probed for polyclonal responses were added to cells and incubated for 1 hour on ice. Following several washes with PBS/1% BSA, cells were incubated for 30 minutes on ice with a 1:1,600 dilution of AlexaFluor647 conjugated $F(ab)_2$ goat anti-mouse IgG Fcγ (Jackson ImmunoResearch). Cells were washed again with PBS/1% BSA and then fixed in 1% formaldehyde in PBS/1% BSA. Cells were analyzed on either a 2 or 4 laser Attune NXT flow cytometer. Data were processed in FlowJo Software.

Immunofluorescence

Cells were seeded to 50% confluency in glass chamber slides (Nunc) and incubated 12–18 hours at 37°C 5% CO_2. Following overnight growth, media from slides were removed and cells were fixed with 4% formaldehyde in PBS (pH 7.4) for 10 minutes at room temperature. Slides were washed in PBS. Diluted commercial antibody (1–4 μg/mL), hybridoma supernatants, or blood serum to be probed for polyclonal responses, were added to the slides and the slides were incubated overnight at 4°C. The slides were washed in PBS and incubated with a 1:800 dilution of AlexaFluor488–conjugated $F(ab)_2$ rabbit anti-mouse IgG (H+L; Invitrogen) for 45 minutes at room temperature. The slides were washed in PBS and mounted using Prolong Gold Antifade Mountant with DAPI (Thermo Fisher Scientific) and examined using an Olympus FV3000 confocal microscope.

IHC

Paraffin-embedded tissue microarrays (TMA) or tissue sections were de-paraffinized with xylene and ethanol, followed by heat-induced antigen retrieval with citrate buffer (pH 6.0) using a microwave oven for 18 minutes. TMAs were stained with Ultra Vison Quanto Detection System HRP DAB. Briefly, TMAs were washed in TBS, incubated with mAb supernatant for 2 hours. After wash in TBS × 2, the TMAs was incubated with Primary Antibody Amplifier Quanto for 10 minutes. After wash in TBS, TMAs were incubated with HRP polymer quanto (10 minutes) followed by DAB chromogen. Slides were counterstained with hematoxylin, dehydrated, and mounted.

CAR T cells

Vector design

A short-chain variable fragment (scFv) was constructed on the basis of 4C8 with V_L and V_H domains linked by a (GGGGS)x3 linker in an LH conformation. This 4C8-scFv was used to generate a second-generation CAR construct, led by a CD8a signal sequence, followed by 4C8-scFv, then a CD8a hinge sequence and CD28 transmembrane domain before ending in the intracellular signaling domains of CD28 and CD3ζ. This 4C8-CAR construct was cloned into the Virapower lentivirus vector pLENTI6.3-V5-DEST (Invitrogen), resulting in the pGO-4C8 transfer vector.

Transduction and expansion

A total of 1×10^6 Lenti-X HEK293T cells (Takara) in a 6-well plate were transfected with pGO-4C8, pCMV-VSV-G (Addgene 8454), and psPAX2 (Addgene 12260) using a 2.6:2.6:1 plasmid ratio, a total of 3.6 μg DNA per well, and 25 μg PEI-40K in 200 μL OptiMEM overnight. The lentiviral supernatant was harvested after 48 hours post transfection. Healthy donor peripheral blood mononuclear cells (PBMC) were isolated by density centrifugation using Lymphoprep followed by depletion of adherent cells. The non-adherent PBMCs were cultured in RPMI-1640 Dutch modification with 10% FBS, 50 μmol/L 2-mercaptoethanol, and 20 ng/mL rIL-2 and were activated using human T-activator CD3/CD28 Dynabeads. The T cells were transduced with viral supernatant 24 hours after activation using spinoculation of 800 × *g* for 30 minutes at room temperature. Transduced 4C8-CAR T cells were expanded in culture medium at densities between a total of 0.5×10^6 cells/mL and 1×10^6 cells/mL until used for experiments.

Cytotoxicity assay

Target cells were seeded at a density of 10,000 per well in 96-well plates and allowed to adhere overnight. 50,000 4C8-CAR T cells were added per well and cell viability was measured over 30 hours by impedance measurements using xCELLigence RTCA eSight. For Jurkat cells, viability was determined using flow cytometry. To assess IFNγ production by the CAR T cells, supernatant was harvested from the co-cultures, and ELISA was performed according to the manufacturer's instructions (R&D Systems).

Organotypic skin tumor model

Organotypic cultures were prepared as described previously (30). Briefly, human fibroblasts were suspended in acid-extracted Type I rat collagen (4 mg/mL) and allowed to polymerize over a 1-mL layer of acellular collagen in 6-well culture inserts with 3 μmol/L pore polycarbonate filters (BD Biosciences). Gels were allowed to contract for 4–5 days before seeding with a total of 3×10^5 N/TERT-1 keratinocytes in DMEM/F12 raft medium supplemented with 1.5% FCS (HyClone), 5 μg/mL insulin (Humulin), 0.1 nmol/L cholera toxin (Sigma), 400 ng/mL hydrocortisone (Sigma), 0.02 nmol/L triiodothyronine, and 0.18 mmol/L adenine (Sigma). To generate invasive growths within an otherwise healthy organotypic skin, hRas-overexpressing N/TERT-1 cells that were genetically modified to express Tn-antigen by KO of the core 1 synthase ($hRas^{KI}$ Core 1^{KO} N/TERT-1) were mixed at different ratios with wild-type N/TERT-1 cells before seeding. Inserts were raised to the air–liquid interface 4 days after seeding keratinocytes, and media were changed every second day for additional 10 days. For experiments using 4C8-CAR T cells, a total of 1×10^6 cells were added directly on top of the organotypic in 10 μL of medium when the inserts were raised to the air–liquid interface. Organotypic sections were prepared and stained histochemically as previously described (30).

In vivo Murine Jurkat model

NSG mice were provided by the University of Pennsylvania Stem Cell and Xenograft Core. Jurkat xenograft models were established by injecting 5 million Click Beetle Green (CBG) luciferase-T2A-GFP–expressing cells in 100 μL of PBS in the lateral tail vein. When the mean total flux of the tumor was between 3.8 and 4.7×10^6 photos/sec, 5 million 4C8 CAR, CD19 CAR, or NTD T cells in 100 μL of PBS, were injected once in the lateral tail vein. CAR T cells were normalized to 82.4% CAR expression. Bioluminescence was measured through serial weekly imaging on a Xenogen IVIS-200 Spectrum camera. Mice were euthanized when moribund or upon the development of hind-limb paralysis. All experiments were performed via protocols approved by the Institutional Animal Care and Use Committee of the University of Pennsylvania.

Statistical analysis

Statistical analysis was conducted in R. Odds ratios and confidence intervals were calculated using logistic regression. ANOVA and/or two-tailed *t* tests were used to test for murine survival and/or cytotoxicity against Tn-positive keratinocytes. *P* values of <0.05 were regarded as statistically significant; *, $P < 0.05$ and **, $P < 0.01$.

Data availability

The data generated in this study are available upon request from the corresponding authors.

Results

mAb 4C8 specifically recognizes Tn-glycosylated CD44v6

To develop a cancer-selective antibody, we immunized mice with a glycopeptide derived from the cancer-associated CD44v6 domain glycosylated with the cancer-associated Tn-epitope (**Fig. 1A**). To identify and target a glycosylation site with high clinical relevance, we combined *O*-glycoproteomics data based on multiple cancer cell lines (36–38) to identify glycosylation sites that are abundantly glycosylated across cancer types and found S422 to be glycosylated in 7 out of 8 cancer cell lines but not in the noncancerous spontaneously immortalized HaCaT keratinocyte cell line (**Fig. 1B**). To generate antibodies against this glycosylation site, we used a murine glycopeptide immunization strategy using an FMOC synthesized glycopeptide [GYRQTPKEDSHS(-Tn)TTGTAAA] carrying Tn-antigen at S12, corresponding to the identified S422 glycosylation site in CD44v6 (**Fig. 1B**). Following hybridoma selection, the mAb 4C8 was found to selectively bind to the Tn-glycosylated CD44v6 peptide and not to non-glycosylated CD44v6 peptide and demonstrated preferential binding to the S12 over the T5 glycosylation site (**Fig. 1C**). Furthermore, 4C8 was found to recognize a wide range of unrelated Tn-glycosylated glycopeptides, though with lower strength than CD44v6-Tn(S12). In

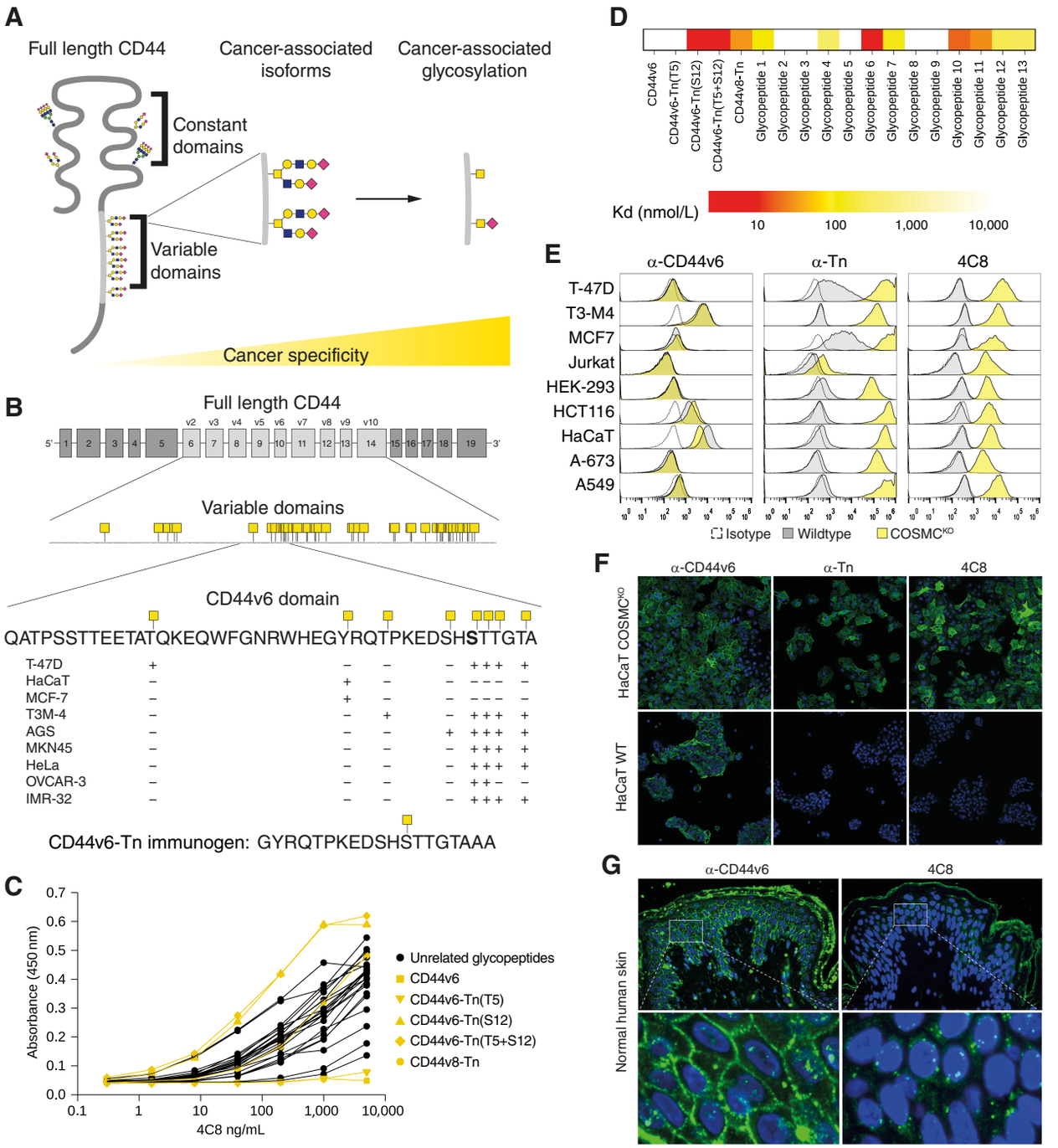

Figure 1.

mAb 4C8 demonstrates high specificity toward CD44v6-Tn. **A,** Schematic illustration demonstrating how increased cancer selectivity can be achieved by targeting cancer-associated glycans within cancer-associated domains of CD44. **B,** Structure of CD44, highlighting the variable region with all its known *O*-glycosylation sites, and then the sequence of the cancer-associated CD44v6 domain likewise with *O*-glycosylation sites highlighted and annotated for which cells lines they have been identified in. **C,** Variable concentrations of 4C8 were used to perform ELISA against non-glycosylated and Tn-glycosylated CD44v6 and unrelated Tn-glycosylated glycopeptides. **D,** Affinities for various Tn-glycosylated glycopeptides, including CD44v6 and naked CD44v6 peptide as measured by Octet. **E,** Various wild-type and COSMC^{KO} cells were stained for flow cytometry using 4C8 and antibodies recognizing Tn-antigen or CD44v6 as controls. Graphs show histograms of cell populations stained with the annotated antibodies. **F,** 4C8 was used to stain wild-type and COSMC^{KO} HaCaT cells for immunofluorescence microscopy. In addition, cells were stained for Tn expression and non-glycosylated CD44v6. Green, CD44v6, Tn, or 4C8, blue, DAPI. **G,** 4C8 was used to stain normal human skin by immunofluorescence. Sections were also stained for non-glycosylated CD44v6. Green, CD44v6 or 4C8, blue, DAPI.

agreement with these results, measurements of the dissociation constant (K_d) using Octet yielded affinities of 6.4 and 7.9 nmol/L for the single and double Tn-glycosylated CD44v6 peptides, respectively, but >10 μmol/L for the T5- and non-glycosylated CD44v6 peptides, whereas 4C8 bound unrelated Tn-glycosylated glycopeptides with affinities ranging from 8.9 to 305 nmol/L (**Fig. 1D**). To assess the specificity of 4C8 in a more natural conformational context, we stained various cancer cell lines as well as HaCaT and HEK293 cells using flow cytometry. To mimic the cancer-associated expression of truncated *O*-glycans in cell lines that are inherently Tn-negative, we used genetic KO of the COSMC chaperone essential for formation of core-1 glycans (25, 43). For Jurkat cells, which are naturally COSMC deficient, we used a COSMC knockin clone as a negative control. When used for flow cytometry, 4C8 selectively stained non-permeabilized COSMC-deficient cells but not their wild-type counterpart (**Fig. 1E**). Expression of CD44v6 was not a predictor for 4C8 binding, as several CD44v6$^-$ cell lines were 4C8$^+$. Instead, we only observed 4C8 reactivity against Tn$^+$ cells and observed no reactivity against Tn$^-$ cells despite CD44v6 expression (**Fig. 1E**). Accordingly, immunofluorescence microscopy of HaCaT cells showed that only Tn$^+$ COSMC^{KO} cells were stained with 4C8 despite expression of CD44v6 in wild-type cells (**Fig. 1F**). As CD44v6 antibodies have previously shown adverse reactions in human skin (40, 41), we used 4C8 to stain normal human skin and importantly observed no 4C8 staining despite CD44v6 expression (**Fig. 1G**). Taken together, these results demonstrate that 4C8 is highly selective for expression of the tumor-associated Tn-antigen, and that although 4C8 binds its target glycopeptide epitope with high affinity, it is also able to recognize a wide range of other glycopeptides in a highly Tn-dependent manner, thereby enabling reactivity against Tn-expressing cancer cell lines that do not express CD44v6.

Cancer-selective reactivity of 4C8 with TMAs

Having demonstrated the Tn-specificity of 4C8, we next examined its cancer selectivity by IHC of human TMAs. Using clear cell surface staining of at least 50% of the tumor tissue as criteria for positive scoring, 4C8 recognized a large proportion of squamous and adenocarcinomas, including colon (∼18%), pancreatic (∼23%), lung (∼31%), and breast carcinomas (∼19%), and showed weak reactivity with prostate carcinomas (**Fig. 2A** and **B**). This finding agrees with the *O*-glycoproteomics data, in which the epitope of 4C8 was found to be expressed across multiple cancer types (**Fig. 1B**). CD44v6 expression was more widespread than 4C8-staining, but although CD44v6 was detected in healthy human tissues, we observed no reactivity with surface structures on healthy human tissues with 4C8, but only occasional intracellular staining of cells particularly of the GI tract (**Fig. 2A–C**). In agreement with the findings presented in **Fig. 1**, tissue reactivity of 4C8 was not necessarily predicted by the presence of CD44v6, as multiple tumors were stained with 4C8 but not for CD44v6. Likewise, several CD44v6$^+$ tumors did not react with 4C8 (**Fig. 2D**). Furthermore, tissue reactivity of 4C8 was highly heterogenous across tumors as demonstrated by wide distribution of H-scores of individually positively scored tumors (**Fig. 2E**), and there was a tendency for decreased reactivity with increasing grade and stage with statistically significant odds ratios for stages 2 and 3 compared with stage 1 when controlled for sex and age (**Fig. 2F**). In conclusion, 4C8 selectively stains tumor tissues from multiple cancers, but not their healthy counterparts, suggesting clinical relevance of the antibody.

Selective cancer killing by glycospecific 4C8 CAR T cells

To further evaluate the clinical potential of 4C8, we designed a 4C8 CAR construct (**Fig. 3A**) and assessed its ability to direct CAR T cells selectively toward cancer cells. Transduced T cells readily expressed 4C8 CAR and selectively targeted COSMC-deficient target cells with minimal reactivity against COSMC-proficient cells (**Fig. 3B** and **C**). 4C8 CAR T cells induced cytotoxicity of COMSC^{KO} HaCaT and HCT-116 cells and showed a strong production of IFNγ, whereas the response against wild-type HaCaT cells was around background levels. 4C8 also targeted wild-type MCF7, which were shown to be partially Tn-positive (**Fig. 1E**), but to a lesser extent. Jurkat cells, which are inherently COSMC-deficient and CD44v6 negative, were also recognized by 4C8 CAR T cells followed by induction of cytotoxicity and IFNγ production, but not upon COSMC^{KI} (**Fig. 3C**). Collectively, these results demonstrate that 4C8 CAR T cells can recognize a range of target cells in a Tn-dependent but CD44v6-independent manner, inducing cytotoxicity that correlates with expression of Tn-antigen in the target cell line.

4C8 CAR T cells induce antitumor response in murine model

Mice were injected with Tn-expressing Jurkat CBG-T2A-GFP cells to establish a xenograft leukemia model with circulating cancer cells. Following treatment with 4C8 CAR T cells, CD19 CAR T cells, or non-transduced T cells, tumor burden was assessed using the CBG luciferase reporter. Treatment with 4C8 CAR T cells, but not the irrelevant CD19 CAR T cells or non-transduced T cells, significantly decreased growth of the Jurkat cells *in vivo* and significantly increased the survival of the mice (**Fig. 4A–C**). In conclusion, these findings show that 4C8 CAR T cells selectively recognize and kill Tn-expressing Jurkat cells *in vivo*, significantly reducing cancer growth and increasing survival.

4C8 CAR T cells in an organotypic skin models indicates improved safety

As immunotherapies targeting CD44v6 have previously shown adverse events in the skin (40, 41), we wanted to examine whether the additional specificity toward the Tn-antigen of 4C8 eliminated cross-reactivities with human skin. In this endeavor, we used a human organotypic skin model, in which N/TERT-1 keratinocytes are grown at the liquid–air interface on top of a fibroblast-embedded collagen matrix. By mixing invasive, hRas-overexpressing N/TERT-1 cells genetically modified to express Tn-antigen by KO of the core 1 synthase instead of its chaperone COSMC (hRas^{KI} Core 1^{KO}) with healthy wild-type N/TERT-1 cells, we created a 3D skin tumor model that we subjected to 4C8 CAR treatment (**Fig. 5A**). 4C8 CAR T cells were able to selectively recognize and kill COSMC^{KO} N/TERT-1 cells in 2D cytotoxicity assays (**Fig. 5B**). In a 3D setting, we found that hRas^{KI} Core 1^{KO} outcompeted the growth of wild-type N/TERT-1 at 1:10 and 1:50 mix ratios, accounting for 50% and 30% of all keratinocytes in the skin, respectively (**Fig. 5C** and **D**). The growth of hRas^{KI} Core 1^{KO} was significantly reduced following treatment with 4C8 CAR T cells, their presence in the organotypic skin practically eliminated, whereas non-transduced T cells has no significant effect (**Fig. 5C** and **D**). Importantly, wild-type keratinocytes formed fully differentiated skin following 4C8 CAR T treatment, with a keratin 5$^+$/keratin 10$^-$ basal layer and keratin 5$^-$/keratin 10$^+$ suprabasal layers, indicating that 4C8 CAR T cells have no adverse cross-reactivities with normal human skin (**Fig. 5C**).

Discussion

In this study, we used *O*-glycoproteomics data from multiple cancer cell lines to identify an abundantly glycosylated serine residue in the cancer-associated CD44v6 domain of CD44 and developed a highly

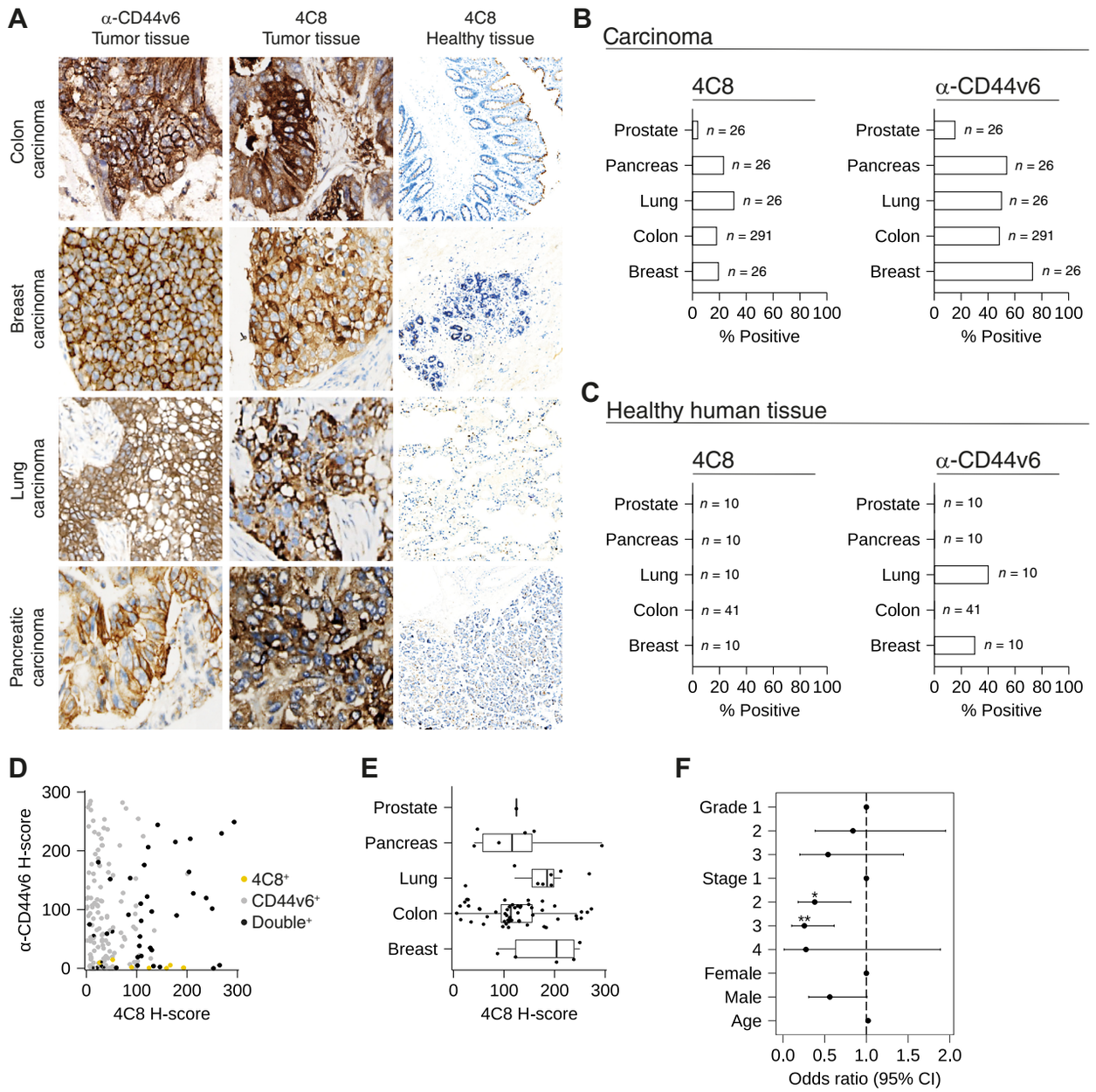

Figure 2.

4C8 selectively stain tumor tissues from several cancers. **A,** 4C8 antibody, anti-CD44 antibody, and IgG isotype control antibody were used to stain tissue microarrays from pancreatic, breast, prostate, colon, and lung carcinomas. Sections show representative stainings of tumor tissue with anti-CD44v6, 4C8, and adjacent normal tissue with 4C8. **B** and **C,** Graphs illustrating the percentage of carcinoma and healthy tissue sections of each tissue type staining positive with 4C8 and non-glycosylated CD44v6. **D,** Dotplot plotting H-scores of 4C8 staining against CD44v6 staining, individual datapoints colored on the basis of scoring as positive for CD44v6 only (gray), 4C8 only (yellow), or both (black). **E,** Boxplots showing distribution of 4C8 H-scores within positively scored tumors. **F,** Odds ratios and 95% confidence intervals for positive 4C8 staining. For cancer grade, odds ratios were calculated compared with grade 1 cancers and were controlled for sex and age. For the cancer stage, odds ratios were calculated compared with stage 1 and were controlled for sex and age. For sex, odds ratios were calculated comparing male with female and were controlled for the grade, stage, and age. For age, odds ratios were controlled for the grade, stage, and sex. *, $P < 0.05$; **, $P < 0.01$.

specific antibody recognizing this Tn-glycosylated site, named 4C8. We demonstrated high specificity of 4C8 against its target, though it also recognized other Tn-glycosylated glycopeptides, and showed high cancer selectivity when staining tissue sections from healthy and tumor tissues by IHC. Furthermore, we showed that 4C8 CAR T cells selectively recognize and kill Tn-expressing cancer cells *in vitro* and significantly reduce cancer growth and increase survival *in vivo* in a murine xenograft model. Finally, we demonstrated that 4C8 CAR T cells can eliminate Tn-expressing cancerous $hRas^{KI}$ Core 1^{KO} N/TERT-1 keratinocytes in a human organotypic skin tumor model, whereas

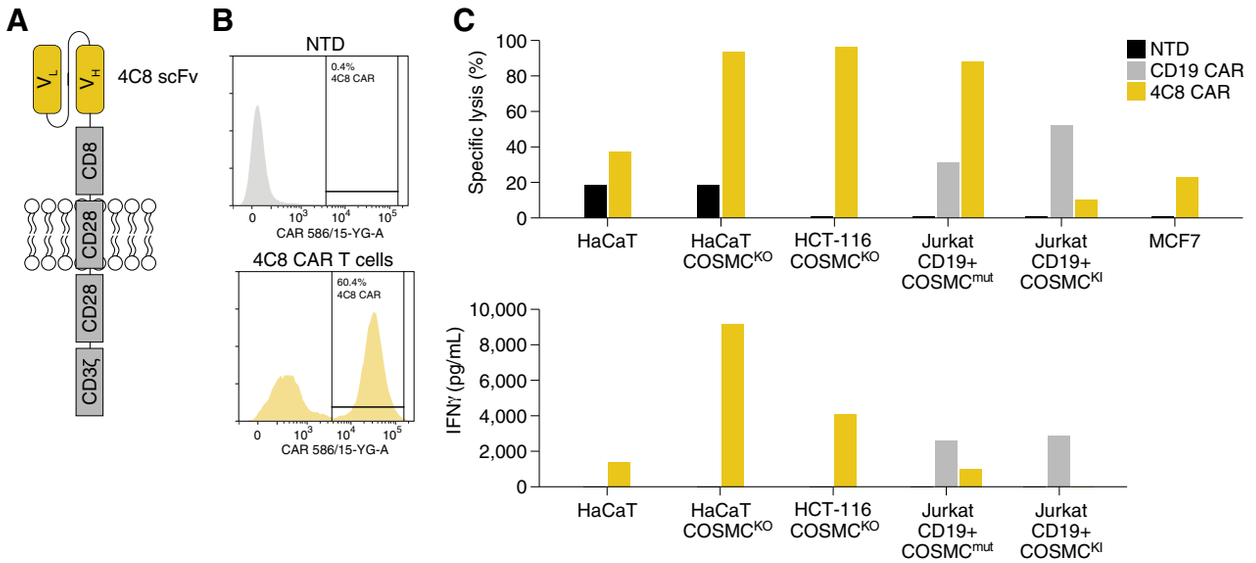

Figure 3.
4C8 CAR T cells selectively kill Tn-expressing cancer cells *in vitro*. **A,** Illustration of the construct design of the 4C8CARs: A single scFv domain derived from 4C8 was joined via the hinge region of CD8 to the transmembrane and intracellular signaling domain of CD28, and finally the intracellular signaling domain of CD3ζ. **B,** Histograms of flow cytometry data showing 4C8 CAR-positive cell populations in non-transduced (NTD) or transduced T cells. **C,** NTD, 4C8 CAR T cells, or CD19 CAR T cells were placed in co-cultures with various target cells, and the target cell viability and the production of IFNγ was measured.

wild-type N/TERT-1 were able to fully differentiate, indicating improved safety in a clinical setting.

One of the big challenges in the field of engineered CAR T-cell therapies for solid tumors has been the identification of safe and universal antigens with high selectivity for cancer cells (6). The selective appearance of truncated *O*-glycans, especially the Tn antigen, on multiple different epithelial-derived human cancers, provides an opportunity to target cancer cells in solid tumors without the inherent problems of adverse events due to reactivity with healthy tissue (7, 9, 10). The presence of the aberrant Tn antigen is a unique feature of cancer cells that can be caused both through direct and indirect mechanisms. Mutations and dysregulation of the enzymes and chaperones controlling O-glycan formation, such as GalNAc transferases, COSMC (*C1GALT1C1*), and C1GalT1 (*C1GALT1*), can all lead to Tn expression (43–52). Although, as demonstrated in The Cancer Genome Atlas, mutations in the COSMC gene are indeed

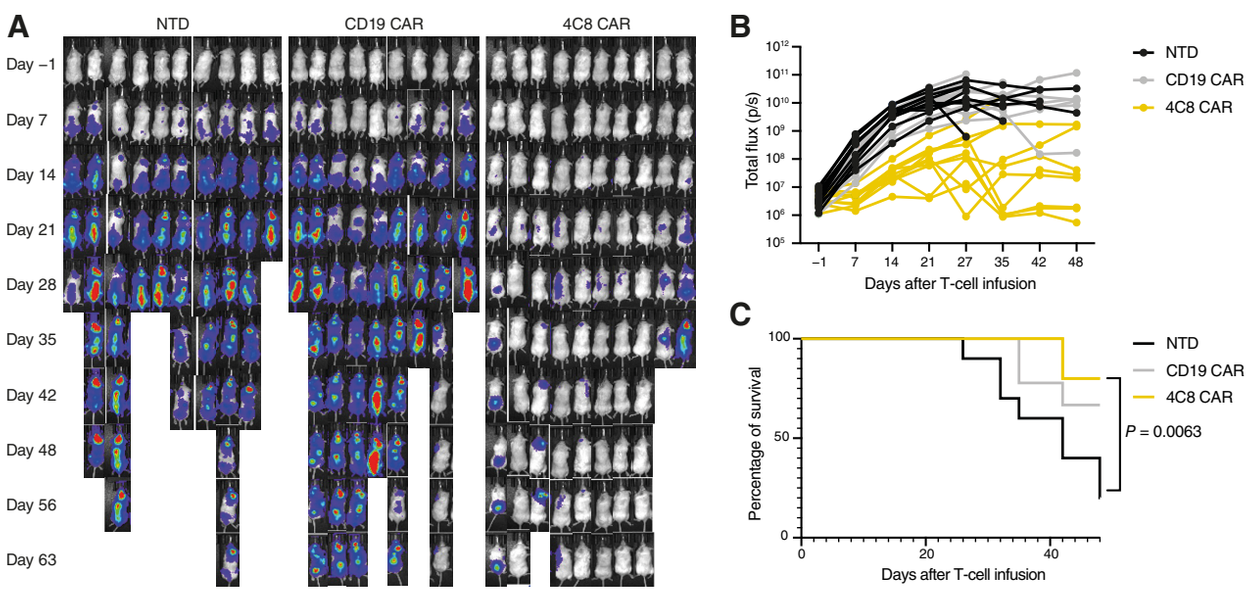

Figure 4.
Jurkat leukemia controlled *in vivo* by 4C8 CAR T cells. **A,** Luminescence images of mice inoculated with Jurkat cells and treated with NTD, CD19, or 4C8 CAR T cells ($n = 10$). **B,** Quantification of luminescence signal from mice. **C,** Survival curve of mice in days after T-cell infusion.

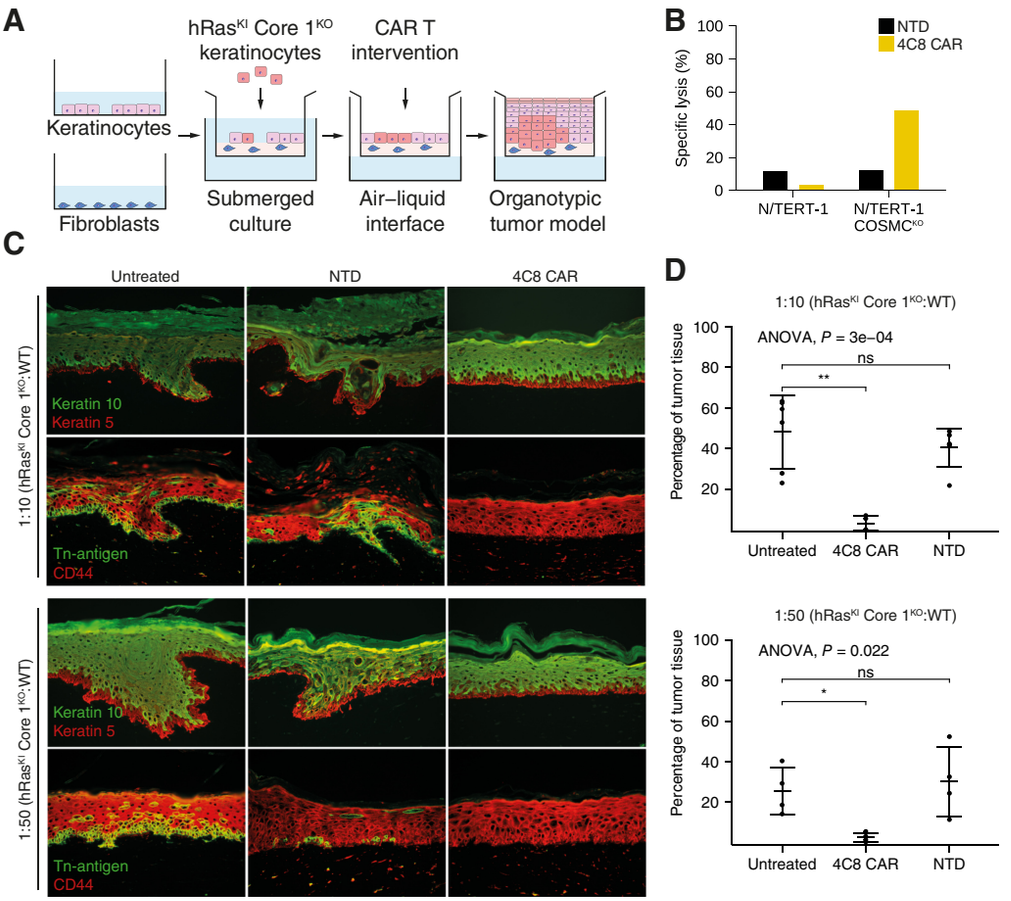

Figure 5.

4C8 CAR T cells show selective killing in organotypic skin tumor model. **A,** Illustration of the experimental setup and production of organotypic skin tumor models. **B,** *In vitro* cytotoxicity of 4C8 CAR T cells against wild-type and COSMC-deficient N/TERT-1 cells. **C,** Immunofluorescence micrographs of sectioned organotypic models stained for Tn-antigen (green) and CD44 (red) or keratin 10 (green) and keratin 5 (red). **D,** Graphs quantifying the percentage of Tn-positive hRas^{KI} Core 1^{KO} keratinocytes in the skin model ($n = 5$). *, $P < 0.05$; **, $P < 0.01$.

found in 1%–6% of human cancers, we have previously shown that it appears epigenetic silencing of the COSMC gene through hypermethylation is an even more common mechanism of Tn expression in cancer, being observed in almost 40% of pancreatic cancers (25, 52). Nevertheless, Tn expression cannot always be ascribed to a direct mechanism, indicating that many cancers express Tn through indirect mechanisms; for example, through dysregulation of pH and organizational changes of the secretory pathway (49, 53, 54). Furthermore, we and others have previously shown that rather than occurring as a side-effect of oncogenesis, Tn expression may itself be involved in driving oncogenesis as its expression directly induces oncogenic features, including dysplastic morphology, increased invasive properties, and decreased cell–cell and cell–matrix adhesion (25–27, 29, 30). Furthermore, the Tn antigen has been shown to modulate immune cell interactions through interactions with the C-type lectin MGL receptor (55–58). Such cancer-promoting effects of truncated O-glycan expression further underscores the potential of using Tn-glycopeptide epitopes in cancer targeting.

CD44 is a heavily glycosylated transmembrane protein that has been suggested as a marker for cancer stem cells (59–61). Efforts have been made to produce antibodies targeting CD44, an example of which is bivatuzumab that recognizes the cancer-associated variable domain CD44v6, but have been shown to cause severe skin toxicities due to a significant expression of CD44v6 in healthy skin (40, 41). The epitope of 4C8 is also localized in the CD44v6 region, but, due to its glycospecific nature, we did not find 4C8 to react with healthy human skin. 4C8 showed a high specificity to Tn-antigen, reacting only with Tn-glycosylated peptides in ELISA and staining only Tn^{+} cells by immunofluorescence and flow cytometry. Although 4C8 had the highest affinity toward its immunogen epitope [fCD44v6-Tn(S12)], it did show some cross reactivity against a wide range of Tn-glycosylated peptides derived from other glycoproteins. In addition, as a CAR T-cell, 4C8 was able to recognize and direct cell-mediated cytotoxicity toward Tn-expressing Jurkat cells in an *in vivo* murine xenograft model despite Jurkat cells expressing no CD44. It therefore seems that the reactivity of 4C8 is dependent on Tn-antigen, whereas its specific affinity toward a Tn-glycosylated epitope is the result of contributions from Tn-antigen and the protein backbone. This makes 4C8 able to recognize a wider range of Tn-glycosylated epitopes while remaining selective for Tn-expressing cells, and not react with any normal human tissues. Other studies have found that antibodies

recognizing Tn-glycosylated MUC1 epitopes, such as AR20.5 and PankoMab, likewise demonstrate a broad but Tn-specific reactivity by recognizing a conformational kink induced by the presence of truncated *O*-glycans in the protein backbone (62–65). It is also possible that conversion to scFv in CAR format has diminished specificity toward its epitope in CD44v6, which would be consistent with previous reports (66, 67). Another explanation is that the high density of CARs on transduced T cells enhances their sensitivity, allowing their recognition of other weak reacting Tn-glycopeptide epitopes (68–71). Nevertheless, this broadening of specificity did not affect the cancer selectivity of the developed CAR T cells, because no reactivity or killing was seen against cells presenting carbohydrate structures beyond the Tn-antigen. It may then be argued that this is a beneficial trait that can address the issues associated with tumor escape by the elimination or downregulation of individual target proteins. Recently, another study by He and colleagues (72) reported a similar effect when adopting their seemingly specific mAb, 237Ab, which recognizes the Tn-glycoform of the mucin-type protein podoplanin. The authors argued that the molecular basis for the broadened Tn selectivity could be explained by previous crystallographic analyses of 237Ab, showing that the antibody enveloped the Tn-antigen inside its binding pocket (73). Hence, and in accordance with our binding data, such Tn-recognizing mAbs are completely dependent on the exposed Tn structure and does not bind to extended *O*-linked glycosylation. The high cancer selectivity of 4C8, as demonstrated by extensive IHC tissue staining, highlights the therapeutic potential of 4C8 and similar Tn-dependent antibodies targeting glycopeptide epitopes.

In conclusion, we have identified a clinically relevant glycopeptide epitope in CD44v6 and generated a cancer-selective and high-affinity mAb against it, named 4C8. 4C8 has high clinical potential for cancer immunotherapies due to its Tn-specific cancer-selective nature, and its safety profile. Moreover, its potential as a potent therapy is shown by its directed cell-dependent cytotoxicity toward Tn-expressing keratinocytes while allowing full differentiation of healthy skin in an organotypic tumor model.

Authors' Disclosures

M.K.M. Aasted reports grants from NEYE foundation during the conduct of the study; personal fees from GO therapeutics outside the submitted work. A.C. Groen reports other support from GO Therapeutics outside the submitted work; as well as reports a patent for anti–glyco-cd44 antibodies and their uses issued; and holds stock in GO Therapeutics. E. Tan reports other support from GO Therapeutics during the conduct of the study; as well as other support from GO Therapeutics outside the submitted work; and reports a patent for PCT/US2021/021211 pending. J. Schnabel reports other support from GO Therapeutics during the conduct of the study; as well as reports a patent for anti–glyco-cd44 antibodies and their uses issued. A.D. Posey Jr reports personal fees from GO Therapeutics during the conduct of the study; and grants and personal fees from Astellas Pharma, personal fees from ImmunoACT, other support from Stromatis Pharma, as well as personal fees from MaxCyte, Iovance, and Mayflower BioVentures outside the submitted work; and reports a patent for US201962824532P pending and a patent for US201962929575P pending. H.H. Wandall reports personal fees from GO therapeutics during the conduct of the study; and other support from Ebumab ApS outside the submitted work; as well as reports a patent for anti–GLYCO-CD44 antibodies and their uses pending. No disclosures were reported by the other authors.

Authors' Contributions

M.K.M. Aasted: Conceptualization, formal analysis, validation, investigation, visualization, methodology, writing–original draft, project administration, writing–review and editing. **A.C. Groen:** Conceptualization, formal analysis, validation, investigation, visualization, methodology, writing–original draft, project administration. **J.T. Keane:** Resources, formal analysis, investigation, methodology. **S. Dabelsteen:** Resources, formal analysis, supervision, investigation, methodology. **E. Tan:** Formal analysis, validation, investigation, methodology. **J. Schnabel:** Formal analysis, validation, investigation, methodology. **F. Liu:** Formal analysis, validation, investigation, methodology. **H.-G.S. Lewis:** Formal analysis, validation, investigation, methodology. **C. Theodoropulos:** Conceptualization, resources, formal analysis, supervision, validation, project administration. **A.D. Posey Jr:** Resources, formal analysis, validation, investigation, methodology. **H.H. Wandall:** Conceptualization, formal analysis, supervision, funding acquisition, validation, methodology, writing–original draft, project administration, writing–review and editing.

Acknowledgments

This work was supported by GO Therapeutics, the Neye Foundation, the European Commission (GlycoSkin H2020-ERC), and the Danish National Research Foundation (DNRF107), The Cancer Research Foundation, Friis Foundation, The Michelsen Foundation, The Danish Research Councils (Sapere Aude Research Leader grant; to H.H. Wandall), A.P. Møller og Hustru Chastine Mc-Kinney Møllers Fond til Almene Formaal, the Lundbeck foundation.

The publication costs of this article were defrayed in part by the payment of publication fees. Therefore, and solely to indicate this fact, this article is hereby marked "advertisement" in accordance with 18 USC section 1734.

Received April 11, 2023; revised June 14, 2023; accepted July 10, 2023; published first July 14, 2023.

References

1. Kochenderfer JN, Wilson WH, Janik JE, Dudley ME, Stetler-Stevenson M, Feldman SA, et al. Eradication of B-lineage cells and regression of lymphoma in a patient treated with autologous T cells genetically engineered to recognize CD19. Blood 2010;116:4099–102.
2. Kalos M, Levine BL, Porter DL, Katz S, Grupp SA, Bagg A, et al. T cells with chimeric antigen receptors have potent antitumor effects and can establish memory in patients with advanced leukemia. Sci Transl Med 2011;3:95ra73.
3. Porter DL, Levine BL, Kalos M, Bagg A, June CH. Chimeric antigen receptor–modified T cells in chronic lymphoid leukemia. N Engl J Med 2011;365:725–33.
4. Brentjens RJ, Davila ML, Riviere I, Park J, Wang X, Cowell LG, et al. CD19-targeted T cells rapidly induce molecular remissions in adults with chemotherapy-refractory acute lymphoblastic leukemia. Sci Transl Med 2013;5:177ra38.
5. Grupp SA, Kalos M, Barrett D, Aplenc R, Porter DL, Rheingold SR, et al. Chimeric antigen receptor–modified T cells for acute lymphoid leukemia. N Engl J Med 2013;368:1509–18.
6. Hou B, Tang Y, Li W, Zeng Q, Chang D. Efficiency of CAR-T therapy for treatment of solid tumor in clinical trials: a meta-analysis. Dis Markers 2019; 2019:3425291.
7. Kudelka MR, Ju T, Heimburg-Molinaro J, Cummings RD. Simple sugars to complex disease—mucin-type o-glycans in cancer. Adv Cancer Res 2015;126: 53–135.
8. Stowell SR, Ju T, Cummings RD. Protein glycosylation in cancer. Annu Rev Pathol Mech Dis 2015;10:473–510.
9. Steentoft C, Migliorini D, King TR, Mandel U, June CH, Posey AD. Glycan-directed CAR-T cells. Glycobiology 2018;28:656–69.
10. Scott E, Elliott DJ, Munkley J. Tumour-associated glycans: a route to boost immunotherapy? Clin Chim Acta 2020;502:167–73.
11. Rømer TB, Aasted MKM, Dabelsteen S, Groen A, Schnabel J, Tan E, et al. Mapping of truncated O-glycans in cancers of epithelial and non-epithelial origin. Br J Cancer 2021;125:1239–50.
12. Munkley J, Elliott DJ. Hallmarks of glycosylation in cancer. Oncotarget 2016;7: 35478–89.
13. Wang M, Zhu J, Lubman DM, Gao C. Aberrant glycosylation and cancer biomarker discovery: a promising and thorny journey. Clin Chem Lab Med 2019;57:407–16.
14. Stanley P. Golgi glycosylation. Cold Spring Harb Perspect Biol 2011;3: a005199.

15. Pinho SS, Reis CA. Glycosylation in cancer: mechanisms and clinical implications. Nat Rev Cancer 2015;15:540–55.
16. Chia J, Goh G, Bard F. Short O-GalNAc glycans: regulation and role in tumor development and clinical perspectives. Biochim Biophys Acta 2016;1860: 1623–39.
17. Wandall HH, Nielsen MAI, King-Smith S, de Haan N, Bagdonaite I. Global functions of O-glycosylation: promises and challenges in O-glycobiology. FEBS J 2021;288:7183–212.
18. Springer GF. Blood group T and Tn antigens are universal, clonal, epithelial cell-adhesive, autoimmunogenic carcinoma markers. Prog Clin Biol Res 1983;133: 157–66.
19. Springer G. T and Tn, general carcinoma autoantigens. Science 1984;224: 1198–206.
20. Julien S, Videira PA, Delannoy P. Sialyl-Tn in cancer: (How) did we miss the target? Biomolecules 2012;2:435–66.
21. Desai PR. Immunoreactive T and Tn antigens in malignancy: role in carcinoma diagnosis, prognosis, and immunotherapy. Transfus Med Rev 2000;14:312–25.
22. Oshikiri T, Miyamoto M, Morita T, Fujita M, Miyasaka Y, Senmaru N, et al. Tumor-associated antigen recognized by the 22–1-1 monoclonal antibody encourages colorectal cancer progression under the scanty $CD8^+$ T cells. Clin Cancer Res 2006;12:411–6.
23. Remmers N, Anderson JM, Linde EM, DiMaio DJ, Lazenby AJ, Wandall HH, et al. Aberrant expression of mucin core proteins and o-linked glycans associated with progression of pancreatic cancer. Clin Cancer Res 2013;19:1981–93.
24. Hofmann BT, Schlüter L, Lange P, Mercanoglu B, Ewald F, Fölster A, et al. COSMC knockdown mediated aberrant O-glycosylation promotes oncogenic properties in pancreatic cancer. Mol Cancer 2015;14:109.
25. Radhakrishnan P, Dabelsteen S, Madsen FB, Francavilla C, Kopp KL, Steentoft C, et al. Immature truncated O-glycophenotype of cancer directly induces oncogenic features. Proc Natl Acad Sci U S A 2014;111:E4066–4075.
26. Bergstrom K, Liu X, Zhao Y, Gao N, Wu Q, Song K, et al. Defective intestinal mucin-type O-glycosylation causes spontaneous colitis-associated cancer in mice. Gastroenterology 2016;151:152–64.
27. Gao N, Bergstrom K, Fu J, Xie B, Chen W, Xia L. Loss of intestinal O-glycans promotes spontaneous duodenal tumors. Am J Physiol Gastrointest Liver Physiol 2016;311:G74–83.
28. Lavrsen K, Dabelsteen S, Vakhrushev SY, Levann AMR, Haue AD, Dylander A, et al. De novo expression of human polypeptide N-acetylgalactosaminyltransferase 6 (GalNAc-T6) in colon adenocarcinoma inhibits the differentiation of colonic epithelium. J Biol Chem 2018;293:1298–314.
29. Bagdonaite I, Pallesen EM, Ye Z, Vakhrushev SY, Marinova IN, Nielsen MI, et al. O-glycan initiation directs distinct biological pathways and controls epithelial differentiation. EMBO Rep 2020;21:e48885.
30. Dabelsteen S, Pallesen EMH, Marinova IN, Nielsen MI, Adamopoulou M, Rømer TB, et al. Essential functions of glycans in human epithelia dissected by a CRISPR-Cas9-engineered human organotypic skin model. Dev Cell 2020;54: 669–84.
31. Nielsen MI, de Haan N, Kightlinger W, Ye Z, Dabelsteen S, Li M, et al. Global mapping of GalNAc-T isoform-specificities and O-glycosylation site-occupancy in a tissue-forming human cell line. Nat Commun 2022;13:6257.
32. Sørensen AL, Reis CA, Tarp MA, Mandel U, Ramachandran K, Sankaranarayanan V, et al. Chemoenzymatically synthesized multimeric Tn/STn MUC1 glycopeptides elicit cancer-specific anti-MUC1 antibody responses and override tolerance. Glycobiology 2006;16:96–107.
33. Wandall HH, Blixt O, Tarp MA, Pedersen JW, Bennett EP, Mandel U, et al. Cancer biomarkers defined by autoantibody signatures to aberrant O-glycopeptide epitopes. Cancer Res 2010;70:1306–13.
34. Posey AD, Schwab RD, Boesteanu AC, Steentoft C, Mandel U, Engels B, et al. Engineered CAR T cells targeting the cancer-associated Tn-glycoform of the membrane mucin MUC1 control adenocarcinoma. Immunity 2016;44: 1444–54.
35. Steentoft C, Fuhrmann M, Battisti F, Van Coillie J, Madsen TD, Campos D, et al. A strategy for generating cancer-specific monoclonal antibodies to aberrant O-glycoproteins: identification of a novel dysadherin-Tn antibody. Glycobiology 2019;29:307–19.
36. Steentoft C, Vakhrushev SY, Vester-Christensen MB, Schjoldager KT-BG, Kong Y, Bennett EP, et al. Mining the O-glycoproteome using zinc-finger nuclease-glycoengineered SimpleCell lines. Nat Methods 2011;8:977–82.
37. Steentoft C, Vakhrushev SY, Joshi HJ, Kong Y, Vester-Christensen MB, Schjoldager KT-BG, et al. Precision mapping of the human O-GalNAc glycoproteome through SimpleCell technology. EMBO J 2013;32:1478–88.
38. King SL, Joshi HJ, Schjoldager KT, Halim A, Madsen TD, Dziegiel MH, et al. Characterizing the O-glycosylation landscape of human plasma, platelets, and endothelial cells. Blood Advances 2017;1:429–42.
39. Heider K-H, Kuthan H, Stehle G, Munzert G. CD44v6: a target for antibody-based cancer therapy. Cancer Immunol Immunother 2004;53:567–79.
40. Tijink BM, Buter J, de Bree R, Giaccone G, Lang MS, Staab A, et al. A phase I dose escalation study with anti-CD44v6 bivatuzumab mertansine in patients with incurable squamous cell carcinoma of the head and neck or esophagus. Clin Cancer Res 2006;12:6064–72.
41. Riechelmann H, Sauter A, Golze W, Hanft G, Schroen C, Hoermann K, et al. Phase I trial with the CD44v6-targeting immunoconjugate bivatuzumab mertansine in head and neck squamous cell carcinoma. Oral Oncol 2008;44:823–9.
42. Prochazka L, Tesarik R, Turanek J. Regulation of alternative splicing of CD44 in cancer. Cell Signal 2014;26:2234–9.
43. Ju T, Cummings RD. A unique molecular chaperone Cosmc required for activity of the mammalian core 1 β3-galactosyltransferase. Proc Natl Acad Sci USA 2002; 99:16613–8.
44. Ju T, Cummings RD. Chaperone mutation in Tn syndrome. Nature 2005;437: 1252.
45. Guo J-M, Chen H-L, Wang G-M, Zhang Y-K, Narimatsu H. Expression of UDP-GalNAc:polypeptide N-acetylgalactosaminyltransferase-12 in gastric and colonic cancer cell lines and in human colorectal cancer. Oncology 2004;67:271–6.
46. Schietinger A, Philip M, Yoshida BA, Azadi P, Liu H, Meredith SC, et al. A mutant chaperone converts a wild-type protein into a tumor-specific antigen. Science 2006;314:304–8.
47. Ju T, Lanneau GS, Gautam T, Wang Y, Xia B, Stowell SR, et al. Human tumor antigens Tn and sialyl Tn arise from mutations in *Cosmc*. Cancer Res 2008;68: 1636–46.
48. Guda K, Moinova H, He J, Jamison O, Ravi L, Natale L, et al. Inactivating germline and somatic mutations in polypeptide *N*-acetylgalactosaminyltransferase 12 in human colon cancers. Proc Natl Acad Sci USA 2009;106:12921–5.
49. Gill DJ, Clausen H, Bard F. Location, location, location: new insights into O-GalNAc protein glycosylation. Trends Cell Biol 2011;21:149–58.
50. Park J-H, Katagiri T, Chung S, Kijima K, Nakamura Y. Polypeptide N-acetylgalactosaminyltransferase 6 disrupts mammary acinar morphogenesis through O-glycosylation of fibronectin. Neoplasia 2011;13:320–6.
51. Taniuchi K, Cerny RL, Tanouchi A, Kohno K, Kotani N, Honke K, et al. Overexpression of GalNAc-transferase GalNAc-T3 promotes pancreatic cancer cell growth. Oncogene 2011;30:4843–54.
52. Mi R, Song L, Wang Y, Ding X, Zeng J, Lehoux S, et al. Epigenetic silencing of the chaperone cosmc in human leukocytes expressing Tn antigen. J Biol Chem 2012; 287:41523–33.
53. Kellokumpu S, Sormunen R, Kellokumpu I. Abnormal glycosylation and altered Golgi structure in colorectal cancer: dependence on intra-Golgi pH. FEBS Lett 2002;516:217–24.
54. Hassinen A, Pujol FM, Kokkonen N, Pieters C, Kihlström M, Korhonen K, et al. Functional organization of Golgi N- and O-glycosylation pathways involves pH-dependent complex formation that is impaired in cancer cells. J Biol Chem 2011; 286:38329–40.
55. Madsen CB, Lavrsen K, Steentoft C, Vester-Christensen MB, Clausen H, Wandall HH, et al. Glycan elongation beyond the mucin associated Tn antigen protects tumor cells from immune-mediated killing. PLoS ONE 2013;8:e72413.
56. Mathiesen CBK, Carlsson MC, Brand S, Möller SR, Idorn M, thor Straten P, et al. Genetically engineered cell factories produce glycoengineered vaccines that target antigen-presenting cells and reduce antigen-specific T-cell reactivity. J Allergy Clin Immunol 2018;142:1983–7.
57. Cornelissen LAM, Blanas A, Zaal A, van der Horst JC, Kruijssen LJW, O'Toole T, et al. Tn antigen expression contributes to an immune suppressive microenvironment and drives tumor growth in colorectal cancer. Front Oncol 2020;10: 1622.
58. Zaal A, Li RJE, Lübbers J, Bruijns SCM, Kalay H, van Kooyk Y, et al. Activation of the C-type lectin MGL by terminal GalNAc ligands reduces the glycolytic activity of human dendritic cells. Front Immunol. 2020;11:305.
59. Prince ME, Sivanandan R, Kaczorowski A, Wolf GT, Kaplan MJ, Dalerba P, et al. Identification of a subpopulation of cells with cancer stem cell properties in head and neck squamous cell carcinoma. Proc Natl Acad Sci U S A 2007;104:973–8.
60. Rajarajan A, Stokes A, Bloor BK, Ceder R, Desai H, Grafström RC, et al. CD44 expression in oro-pharyngeal carcinoma tissues and cell lines. PLoS ONE 2012;7: e28776.
61. Thapa R, Wilson GD. The importance of CD44 as a stem cell biomarker and therapeutic target in cancer. Stem Cells Int 2016;2016:2087204.

62. Karsten U. Binding patterns of DTR-specific antibodies reveal a glycosylation-conditioned tumor-specific epitope of the epithelial mucin (MUC1). Glycobiology 2004;14:681–92.
63. Karsten U, von Mensdorff-Pouilly S, Goletz S. What makes MUC1 a tumor antigen? Tumor Biol 2005;26:217–20.
64. Danielczyk A, Stahn R, Faulstich D, Löffler A, Märten A, Karsten U, et al. PankoMab: a potent new generation antitumour MUC1 antibody. Cancer Immunol Immunother 2006;55:1337–47.
65. Movahedin M, Brooks TM, Supekar NT, Gokanapudi N, Boons G-J, Brooks CL. Glycosylation of MUC1 influences the binding of a therapeutic antibody by altering the conformational equilibrium of the antigen. Glycobiology 2017;27:677–87.
66. Glazer AN. On the prevalence of "nonspecific" binding at the specific binding sites of globular proteins. Proc Natl Acad Sci USA 1970;65:1057–63.
67. Richards FF, Konigsberg WH, Rosenstein RW, Varga JM. On the specificity of antibodies: biochemical and biophysical evidence indicates the existence of polyfunctional antibody combining regions. Science 1975;187:130–7.
68. Purbhoo MA, Irvine DJ, Huppa JB, Davis MM. T-cell killing does not require the formation of a stable mature immunological synapse. Nat Immunol 2004;5:524–30.
69. Huse M, Klein LO, Girvin AT, Faraj JM, Li Q-J, Kuhns MS, et al. Spatial and temporal dynamics of T-cell receptor signaling with a photoactivatable agonist. Immunity 2007;27:76–88.
70. Huang J, Brameshuber M, Zeng X, Xie J, Li Q, Chien Y, et al. A single peptide-major histocompatibility complex ligand triggers digital cytokine secretion in $CD4^+$ T cells. Immunity 2013;39:846–57.
71. Han A, Glanville J, Hansmann L, Davis MM. Linking T-cell receptor sequence to functional phenotype at the single-cell level. Nat Biotechnol 2014;32:684–92.
72. He Y, Schreiber K, Wolf SP, Wen F, Steentoft C, Zerweck J, et al. Multiple cancer-specific antigens are targeted by a chimeric antibody receptor on a single cancer cell. JCI Insight 2019;4:e130416.
73. Brooks CL, Schietinger A, Borisova SN, Kufer P, Okon M, Hirama T, et al. Antibody recognition of a unique tumor-specific glycopeptide antigen. Proc Natl Acad Sci USA 2010;107:10056–61.